Journal of Solid State Chemistry 183 (2010) 1365–1371

Contents lists available at ScienceDirect

Journal of Solid State Chemistry

journal homepage: www.elsevier.com/locate/jssc

Preparation of three-dimensionally ordered macroporous perovskite-type lanthanum–iron-oxide $LaFeO_3$ with tunable pore diameters: High porosity and photonic property

Masahiro Sadakane *, Toshitaka Horiuchi, Nobuyasu Kato, Keisuke Sasaki, Wataru Ueda *,[1]

Catalysis Research Center, Hokkaido University, N-21, W-10, Sapporo 001-0021, Japan

ARTICLE INFO

Article history:
Received 30 November 2009
Received in revised form
4 April 2010
Accepted 11 April 2010
Available online 28 April 2010

Keywords:
Macroporous material
Template method
Colloidal crystal
Perovskite
Photonic crystal

ABSTRACT

Three-dimensionally ordered macroporous (3DOM) lanthanum–iron-oxide ($LaFeO_3$) with different pore diameters was prepared using a colloidal crystal of polymer spheres with different diameters as templates. Ethylene glycol–methanol mixed solution of metal nitrates was infiltrated into the void of the colloidal crystal template of a monodispersed poly(methyl methacrylate) (PMMA) sphere. Heating of this PMMA–metal salt–ethylene glycol composite produced the desired well-ordered 3DOM $LaFeO_3$ with a high pore fraction, which was confirmed by powder X-ray diffraction (XRD), scanning electron microscopy (SEM), transmission electron microscopy (TEM), mercury (Hg) porosimetry, and ultraviolet–visible (UV–vis) diffuse reflectance spectra. 3DOM $LaFeO_3$ with pore diameters of 281 and 321 nm shows opalescent colors because of photonic stop band properties. Catalytic activity of the 3DOM $LaFeO_3$ for combustion of carbon particles was enhanced by a potassium cation, which was involved from $K_2S_2O_8$ used as a polymerization initiator.

1. Introduction

Perovskite-type iron (Fe) and lanthanum (La) mixed metal oxides, $LaFeO_3$, have attracted much attention as oxidation catalysts, sensors, and electrode materials [1–5]. The most common method for preparing $LaFeO_3$ is a solid state reaction between the component metal oxides or carbonates, and this method requires a calcination temperature higher than 1273 K to obtain the desired product as a single phase, which results in reduction in surface area (usually less than $1\,m^2\,g^{-1}$) due to large crystal sizes. Increase in specific surface area, i.e., decrease in particle sizes, is desired to enhance performance of their application.

In order to increase the specific surface area, so-called wet-chemical procedures, including thermal decomposition of precipitated precursors [2,6,7], a microemulsion method [8], and pyrolysis of complex precursor [9,10], have been reported. In these methods, lanthanum and iron precursors are dissolved in a solvent and homogeneous mixing of metals is ensured, thus reducing calcination temperature to form the desired $LaFeO_3$. Nano-crystalline $LaFeO_3$ can be formed and specific surface area can be increased. If crystallite size of $LaFeO_3$ is 30 nm, specific surface area is calculated to be $30\,m^2\,g^{-1}$ [11]. Thus, produced materials are aggregates of nano-particles.

Recently, much attention has been focused on three-dimensionally ordered macroporous (3DOM) materials with pores sized in the sub-micrometer range because of their application in photonic crystals, catalysis, and separation [12,13]. 3DOM materials are produced by the following procedure: (i) a colloidal crystal template is prepared by ordering monodisperse spheres, e.g., polystyrene, poly(methyl methacrylate) or silica, into a face-centered close-packed array (opal structure), (ii) interstices in the colloidal crystal are then filled with liquid metal precursors, either neat or in solution, which solidify in voids of sphere templates, resulting in an intermediate composite structure, and (iii) an ordered form is produced after removing the template by calcination or extraction. The ordered (“inverse opals”) structures synthesized using this method consists of a skeleton surrounding uniform close-packed macropores. The macropores are interconnected through windows that form as a result of contact between the template spheres prior to infiltration of the precursor solution. Furthermore, the 3DOM materials have high porosity, theoretically ca. 74%.

We have been interested in preparing 3DOM $LaFeO_3$, because the 3D macropores together with high porosity can permit more facile transport of guest molecules and ions compared to

* Corresponding author. Present address: Chemistry and Chemical Engineering, Graduate School of Engineering, Hiroshima University, 1-4-1, Kagamiyama, Higashi-Hiroshima, Hiroshima 739-8527, Japan. Fax: +81 82 424 5494.
* Corresponding author.
E-mail addresses: sadakane09@hiroshima-u.ac.jp (M. Sadakane), ueda@cat.hokudai.ac.jp (W. Ueda).
[1] Fax: +81 11 706 9163.

0022-4596/$ - see front matter © 2010 Elsevier Inc. All rights reserved.
doi:10.1016/j.jssc.2010.04.012

aggregates of nano-particles prepared using the usual wet-chemical procedure, which is attractive for catalysis materials and electrode materials. Furthermore, regular 3D periodicity with a distance of several hundred nanometers is attractive for photonic crystal materials.

However, it has been difficult to prepare 3DOM $LaFeO_3$ using conventional sol–gel methods or precipitation methods, and we have therefore developed a facile method for production of 3DOM $LaFeO_3$ using a colloidal crystal template of poly(styrene) [14]. We used an ethylene glycol (EG)–methanol mixed solution of metal nitrate salts, which can be converted to a mixed metal glyoxylate or metal oxalate derivatives by *in-situ* nitrate oxidation at a low temperature before removal of the template. Further calcination removed the polymer template and converted the glyoxylate salt to mixed metal oxide, resulting in production of 3DOM mixed iron oxide materials in high yield. This *in-situ* solidification ensures the chemical homogeneity of the product. However, pore structure was poorly ordered.

We later found that poly(methyl metacrylate) (PMMA) is a better template material, and we reported in our previous communication that well-ordered 3DOM $LaFeO_3$ can be produced [15].

In this paper, we describe the preparation and structural characterization of 3DOM $LaFeO_3$ with different pore diameters using PMMA templates with different sphere diameters.

2. Experimental

2.1. Materials

All chemicals used were of reagent grade and they were used as supplied. Suspensions of monodisperse poly(methyl methacrylate) (PMMA) spheres (diameters: 183 ± 6, 268 ± 9, and 413 ± 15 nm) were synthesized using potassium peroxosulfate as a polymerization initiator by literature techniques [16]. Suspensions of monodisperse poly(methyl methacrylate) (PMMA) spheres (diameters: 277 ± 8 and 444 ± 12 nm) were synthesized using 2,2′-azobis(2-methylpropionamidine) dihydrocholoride as a polymerization initiator by literature techniques [17]. These spheres were packed into colloidal crystals by centrifugation. The obtained template was crushed with an agate mortar and the obtained particles were adjusted to 0.425–2.000 mm in size using testing sieves (Tokyo Screen, Co. Ltd.) [16,18]. Quartz sand (10–15 mesh) was purchased from Kokusan Chemical Works (Tokyo).

2.2. Characterizations

Powder X-ray diffraction (XRD) patterns were recorded on a diffractometer (Rigaku, RINT Ultima+) equipped with a graphite monochromator using Cu$K\alpha$ radiation (tube voltage: 40 kV, tube current: 20 mA). The diffraction line widths were obtained after subtraction of the instrumental width determined by the line width of silicon powder, and crystallite sizes were calculated from the width of the most intense lines using the Scherrer equation. Cell parameters were calculated using a least-squares method from 6 XRD lines. Scanning electron microscopy (SEM) images were obtained with a JSM-7400F (JEOL). Samples for SEM were dusted on an adhesive conductive carbon paper attached to a brass mount. Transmission electron microscopy (TEM) images were obtained with a JEM-2000FX (JEOL) using accelerating voltage of 200 kV with LaB_6 filament. Samples for TEM were prepared by sonicating small amounts of the powder in 5 ml of ethanol for 1 min and then depositing a few drops of the suspension on a holey carbon grid. Nitrogen adsorption measurements were performed on an Autosorb 6 (Quantachrome, USA) sorption analyzer. Prior to the sorption measurements, the samples were degassed under vacuum at 473 K for 1 h. Surface areas were calculated by the Brunauer–Emmet–Teller (BET) method. Meso and macropores were characterized by an Hg porosimetry experiment using PoreMaster 33P (Quantachrome, USA). Pore sizes were calculated using the Washburn equation with an Hg contact angle of 140° and a surface tension of 480 dyne cm^{-1}. Diffuse-reflectance (DR) UV–vis spectra were obtained on a JASCO V-570 spectrophotometer equipped with an ISN-470 reflectance spectroscopy accessory. Samples were randomly oriented bulk powders. Elemental analyses were carried out by Mikroanalytisches Labor Pascher (Remagen, Germany).

2.3. Synthesis of 3DOM $LaFeO_3$

Lanthanum nitrate hydrate ($La(NO_3)_3 \cdot 6H_2O$, 10.8 g) and iron nitrate hydrate ($Fe(NO_3)_3 \cdot 9H_2O$, 10.1 g) (final metal concentration: 2 M) were dissolved with ca. 5 mL of ethyleneglycol (EG) by slow stirring in a 100 mL beaker at room temperature until the nitrate salt had dissolved, and the produced EG solution was poured into a 25 mL volumetric flask. Methanol (10 mL) and EG were added in amounts necessary to achieve the desired concentration (final concentration of methanol being 40% of the volume). Then the PMMA colloidal crystals were soaked in the solution for 3 h. Excess solution was removed from the impregnated PMMA colloidal crystals by vacuum filtration. The obtained sample was allowed to dry in air at room temperature overnight. A 0.5 g amount of the sample was mixed with 2.5 g of quartz sand (10 − 15 mesh) and calcined in a tubular furnace (inner diameter of ca. 21 mm) in an air flow (50 mL min^{-1}). The temperature was raised at a rate of 1 K min^{-1} to 873 K and held for 5 h.

3DOM $LaFeO_3$ materials were prepared using PMMA templates with different diameters. PMMA templates with diameters of 183, 268, 291 and 413 nm prepared using a potassium peroxosulfate polymerization initiator and PMMA template with diameters of 277 and 444 nm prepared using a 2,2′-azobis(2-methylpropionamidine) dihydrocholoride polymerization initiator were denoted as 3DOM-PPS-183, 3DOM-PPS-268, 3DOM-PPS-291, 3DOM-PPS-413, 3DOM-AMPD-277, and 3DOM-AMPD-444, respectively.

2.4. Synthesis of nonporous $LaFeO_3$

The EG − methanol solution of the mixed La–Fe nitrate was heated in a muffle oven at a rate of 1 K min^{-1} to 473 K. A 0.5 g amount of the produced solid was calcined in a tube furnace with an air flow (50 mL min^{-1}). The temperature was raised at a rate of 1 K min^{-1} to 873 K and held for 5 h.

2.5. Synthesis of nonporous $LaFeO_3$-K (K: ca. 0.08 wt%)

The EG − methanol solution (10 mL) of the La–Fe nitrate was mixed with aqueous solution (200 μL) of K_2SO_4 (8.7 mg), and this solution was heated in a muffle oven at a rate of 1 K min^{-1} to 473 K. A 0.5 g amount of the produced was calcined in a tube furnace with an air flow (50 mL min^{-1}). The temperature was raised at a rate of 1 K min^{-1} to 873 K and held for 5 h.

2.6. Catalytic tests

Catalytic activity of the prepared materials was tested in a TG-DTA apparatus. A 20 mg amount of the prepared materials was soaked in 25 mL of the carbon particle colloidal solution

(Nanoamand, NanoCarbon Research Institute Ltd., nanoscale diamond (diameter < 10 nm) colloid dispersed in ethanol) diluted with 625 mL of ethanol and ultrasonicated for 5 min. The solution was dried at 353 K for 1 h and the obtained 1:10 by weight mixture (10 mg) of carbon and catalyst was heated in a TG-DTA apparatus under air flow (50 mL min^{-1}).

3. Results and discussion

3.1. Preparation and structural characterization of 3DOM $LaFeO_3$ with different pore sizes

In our previous communication [15], we described the preparation of 3DOM $LaFeO_3$ using a colloidal crystal template of PMMA with a diameter of 291 nm (Entry 3, Table 1). Well-ordered 3DOM $LaFeO_3$ with a pore size of 198 nm was obtained.

PMMA spheres with different diameters ranging from 183 to 444 nm were prepared using potassium peroxosulfate (PPS) or 2,2′-azobis(2-methyl propionamidine) dihydrochloride (AMPD) as a polymerization initiator. These PMMA spheres were packed into a colloidal crystal and tested as templates. Ethylene glycol–methanol mixed solution of lanthanum nitrate and iron nitrate was infiltrated in the void of the PMMA colloidal crystal template. After calcination at 873 K, the obtained solid was characterized using SEM, TEM, XRD and N_2-adsorption, and data are summarized in Table 1.

A well-ordered 3DOM structure was obtained for all samples, as shown in SEM images in Fig. 1. Well-ordered air spheres and interconnected walls created an "inverse opal" structure in three dimensions, and the next layer is clearly visible in the SEM images. Large fractions (more than 95% of the particles by SEM images) of all of the 3DOM materials were highly ordered porous structures in three dimensions over a range of tens of micrometers.

It is known that polymerization initiators exist on the surface of PMMA [19]. These PMMA polymerization initiators did not affect formation of the 3DOM structure. However, potassium and sulfur (Entries 1–3 and 4) or chlorine (Entries 5 and 6) from the initiator remained in the sample after calcination.

The production of $LaFeO_3$ was confirmed by XRD measurement (Fig. 2) with reference to JCPDS data bank 37-1493. The cell parameters were very similar to the reported values (Table S1). Furthermore, no by-products were detected, indicating that the desired $LaFeO_3$ was successfully obtained. Crystallite sizes estimated from XRD were 26–36 nm, which correspond to wall widths.

The 3DOM structure was characterized in more detail using TEM (Fig. 3). The 3DOM structure of crystalline materials is a so-called skeleton structure that consists of strut-like bonds and vertices [16,18,20,21]. The struts connect two kinds of vertices and form a CaF_2 lattice, in which the eight-coordinated square prism calcium vertex is larger than the tetrahedral fluorine vertex. Pore sizes corresponding to the distance between the centers of two neighboring open spheres were estimated from TEM images (Fig. 3(a)). Pore sizes are always ca. 30% smaller than the original PMMA sphere diameter, mostly due to melting shrinkage of the PMMA sphere [16]. The pore was surrounded by 12 rhombic windows, and the long diagonal distance and short diagonal distance of the window were also estimated from TEM images. Window sizes and pore sizes were increased by increasing the PMMA sphere diameter.

In the case of 3DOM spinel iron oxide, MFe_2O_4 (*M*: Ni, Zn, and Co), we have observed additional voids in the eight-coordinated square prism vertices [16]. In the case of 3DOM $LaFeO_3$, voids were observed both in struts and vertices, as indicated by arrows in Fig. 3(b).

Fig. 3(c) and (d) show TEM images of 3DOM-PPS-268 obtained after calcination at 473 and 673 K, respectively. These products were amorphous compounds. After calcination at 473 K, PMMA still remained and a 3DOM structure in the polymer was clearly seen (Fig. 3(c)), and additional voids in the square prism vertices were observed. After calcination at 673 K, the polymer was removed and a 3DOM structure was observed, and additional voids in the square prism vertices and struts were clearly observed. Swelling of the voids in the square prism vertices was observed at this temperature. The swollen vertices were shrunk by crystallization at a higher temperature.

3.2. Porosity

Porosity was measured using Hg porosimetry [16]. The incremental intrusion was plotted against pore diameter for 3DOM-PPS-268 and $LaFeO_3$ prepared without a PMMA template (Fig. 4). The Hg intrusion in the low-pressure region (ca. 0.1–10 μm) is due to the interparticle voids and cracks in the particles, which are observed on the surface of particles (for example, Fig. 1(a) and (c)). The sharp increase in Hg intrusion (the peak top: 79 nm) is due to the interconnecting windows between macropores (Fig. 4, closed circles), and this value is similar to the window sizes (70–65 nm) estimated by TEM (Entry 2).

Additional voids in 3DOM struts and vertices were not detected by Hg porosimetry, indicating that the additional voids were closed and not accessible.

Table 1
Physicochemical properties of 3DOM $LaFeO_3$ prepared using different polymer templates

Entry	Sample	Initiator[b]	PMMA diameter (nm)	Pore size (nm)[c]	Window size (nm)[c]	BET surf. area ($m^2 g^{-1}$)	Crystallite size (nm)[d]	Impurity (wt%)	T_{20} (K)[e]
1	3DOM-PPS-183	PPS	183 ± 6	127	65 × 56	30	36	K: 0.1 S: 0.2	468
2	3DOM-PPS-268	PPS	268 ± 9	165	70 × 65	26	26	K: 0.2 S: 0.3	489
3	3DOM-PPS-291[a]	PPS	291 ± 8	198	n.d.		25		
4	3DOM-PPS-413	PPS	413 ± 15	281	98 × 89	23	36	K: 0.02 S: 0.2	501
5	3DOM-AMPD-277	AMPD	277 ± 8	n.d.	n.d.	32	33	Cl: 0.05	519
6	3DOM-AMPD-444	AMPD	444 ± 12	321	n.d.	29	30	Cl: 0.05	523
7	Non-porous $LaFeO_3$					21	36		523
8	Non-porous $LaFeO_3$-K					28	46		463

[a] Data in our previous paper [14].
[b] PPS: potassium peroxosulfate, $K_2S_2O_8$, AMPD: 2,2′-azobis(2-methyl propionamidine) dihydrochloride.
[c] Pore sizes and window sizes were estimated from the (110) direction of TEM images.
[d] Crystallite sizes were calculated by Scherrer's equation from XRD data.
[e] Carbon particle combustion temperature. T_{20} is a temperature where 20 wt% of the carbon was burned.

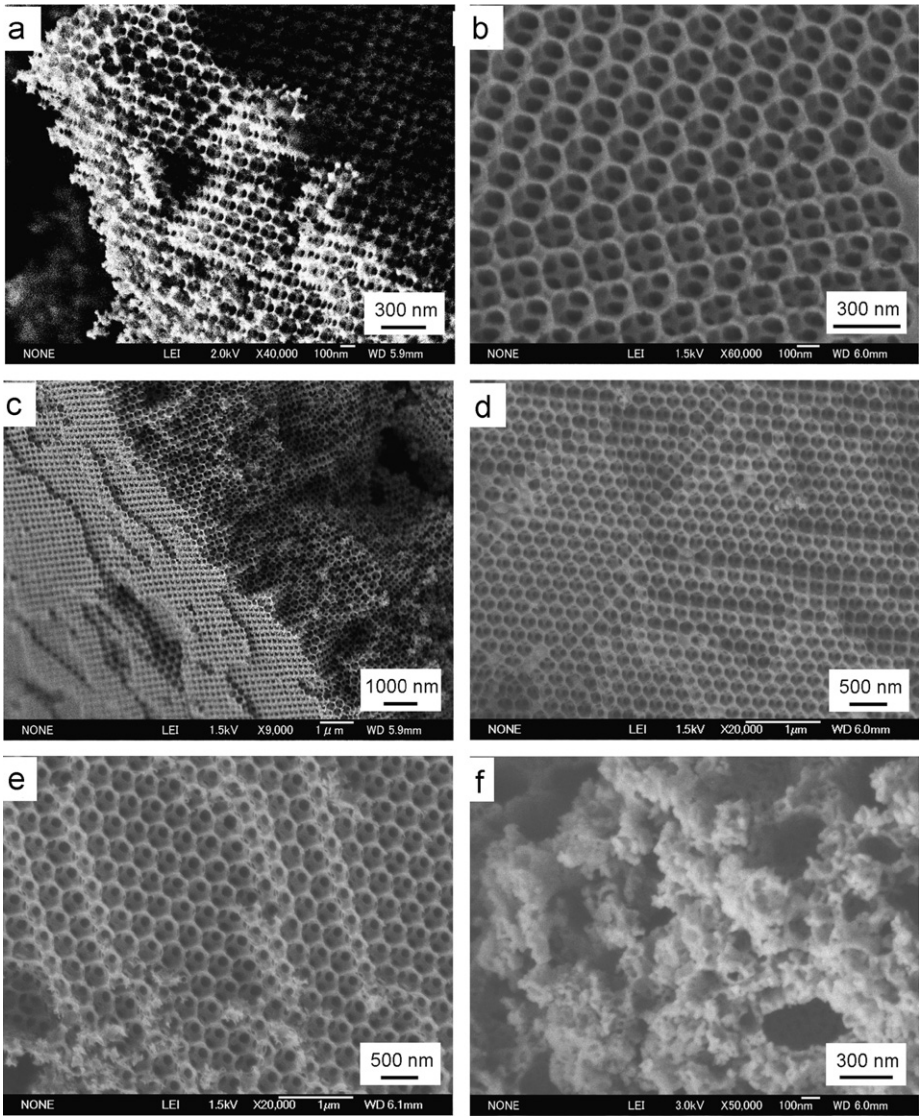

Fig. 1. SEM images of 3DOM $LaFeO_3$ prepared using colloidal crystal templates of PMMA($K_2S_2O_8$-183 nm), 3DOM-PPS-183 (a), PMMA($K_2S_2O_8$-268 nm), 3DOM-PPS-268 (b), PMMA($K_2S_2O_8$-413 nm), 3DOM-PPS-413 (c), PMMA(AMPD-277 nm), 3DOM-AMPD-277 (d), PMMA(AMPD-444 nm), 3DOM-AMPD-444 (e), and non-porous $LaFeO_3$ prepared without a PMMA template (f).

Porosity was calculated by the amount of intrusion Hg in the macropore [16]. The calculated porosity of 3DOM-PPS-268 was 80%, which is close to the theoretical value (74%) of porosity of inverse opals. This result indicates that samples made by our method have the desired 3DOM structure quantitatively.

In the case of non-porous $LaFeO_3$, most of the pore sizes were within the range of ca. 0.1–10 μm, corresponding to pores between aggregates of nano-particles (Figs. 1(f) and 3(e)). A small peak centered at 31 nm corresponds to pore sizes between nano-particles in aggregates. These results demonstrate that 3DOM $LaFeO_3$ had high porosity with uniform connecting pore sizes, which is an attractive feature for potential catalysts, filter materials, and electrode materials.

3.3. Photonic properties

The color of $LaFeO_3$ is brown, but 3DOM-PPS-413 and 3DOM-AMPD-444 appeared opalescent green and orange, respectively, under room light (Fig. 5). The 3DOM $LaFeO_3$ were characterized by using DR UV–Vis spectroscopy (Fig. 6), and a photonic stop band centered at 494 or 600 nm corresponding to green or orange color, respectively, were observed.

An approximate expression for the position of the stop band is given by

$$\lambda = 2d_{hkl}n_{avg}, \quad (1)$$

where λ is the wavelength of the stop band minimum, d_{hkl} is the interplanar spacing, and n_{avg} is the average refractive index of the materials [12,22]. The n_{avg} is given by

$$n_{avg} = \{(1-a)n_{wall}^2 + an_{void}^2\}^{1/2}, \quad (2)$$

where a is pore fraction of the material, n_{wall} is refractive index of $LaFeO_3$, and n_{void} is refractive index of air (n_{void}=1.00). The interplanar spacing of the (111) sets planes d_{111} is given by

$$d_{111} = (2/3)^{1/2}D, \quad (3)$$

where D is pore size. Calculated n_{avg} of 3DOM-PPS-413 and 3DOM-AMPD-444 are 1.08 and 1.14, respectively. We propose that this small difference is caused by difference of pore fraction between 3DOM-PPS-413 and 3DOM-AMPD-444. There have been a lot of publications about photonic stop band of 3DOM metal

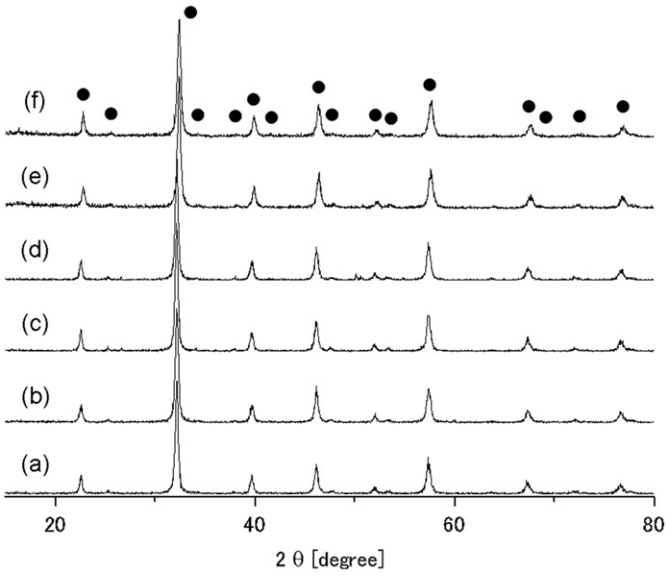

Fig. 2. XRD of non-porous $LaFeO_3$ prepared without a PMMA template (a), 3DOM-PPS-183 (b), 3DOM-PPS-268 (c), 3DOM-PPS-413 (d), 3DOM-AMPD-277 (e), and 3DOM-AMPD-444 (f).

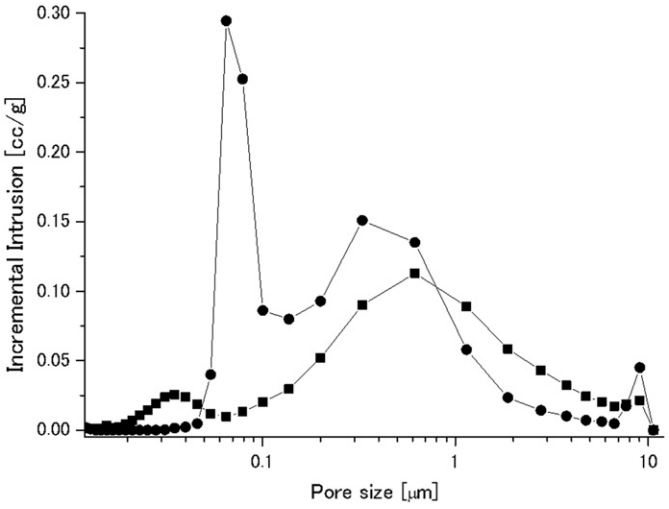

Fig. 4. Incremental intrusion spectra of Hg porosimetry of 3DOM-PPS-268 (closed circles) and non-porous $LaFeO_3$ prepared without a PMMA template (closed squares).

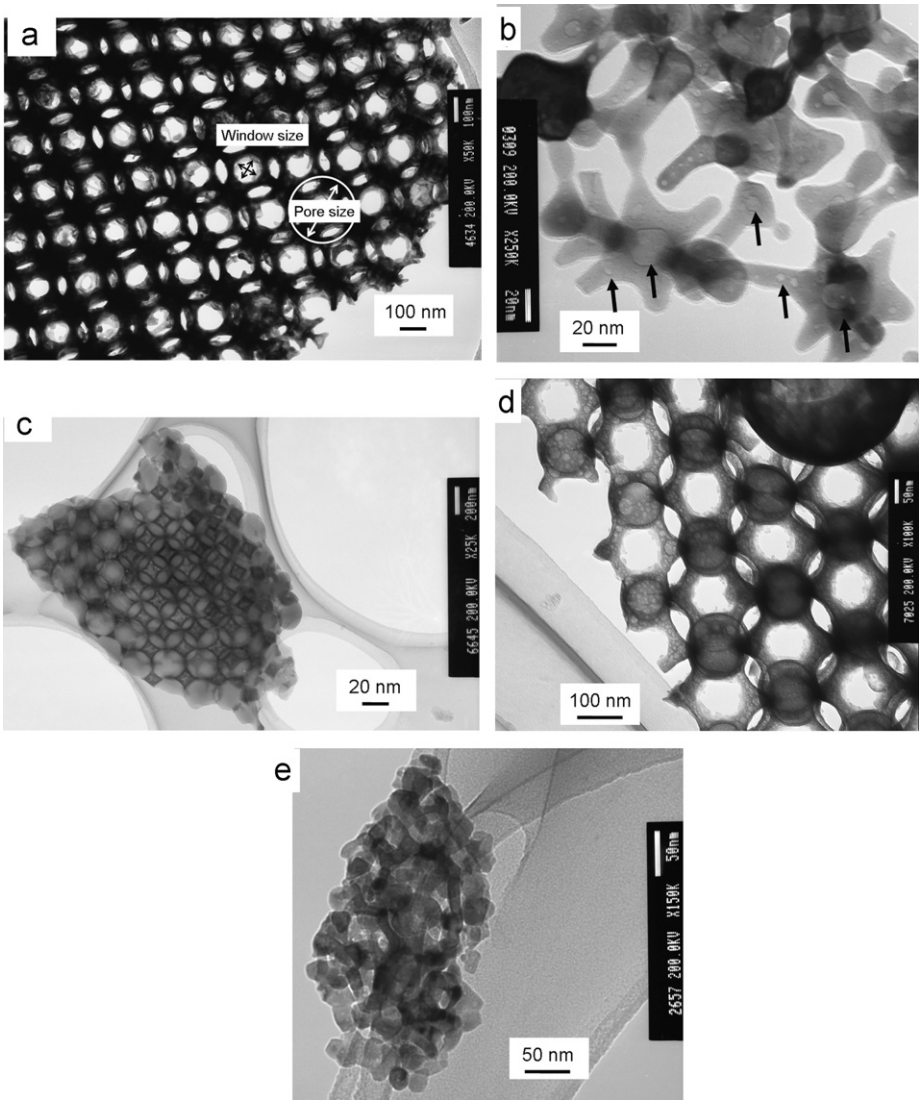

Fig. 3. TEM images of 3DOM-PPS-268. Calcination temperatures were 873 K (a) and (b), 473 K (c), and 673 K (d). View toward the (100) plane. Arrows show pore size and window size (a) and arrows in (b) indicate additional voids. TEM image of non-porous $LaFeO_3$.

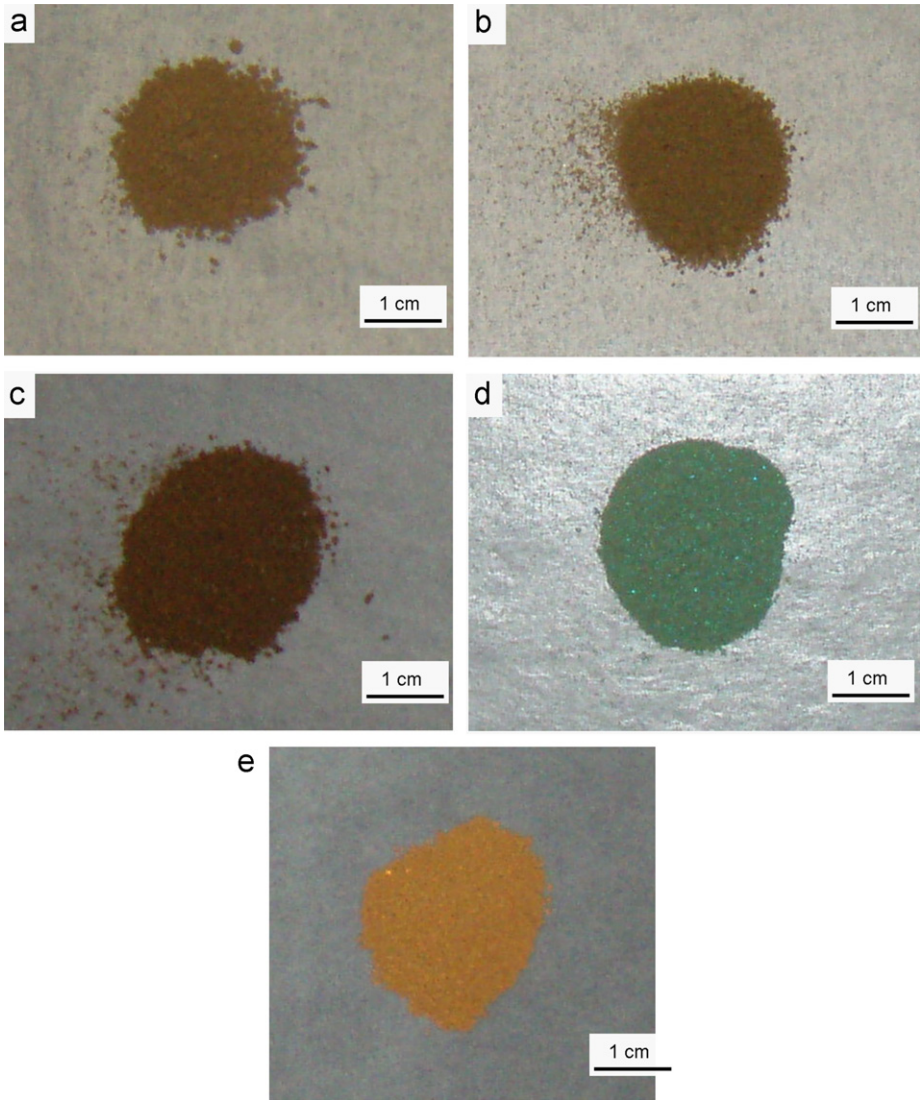

Fig. 5. Photographs of non-porous $LaFeO_3$ prepared without a PMMA template (a) and with PMMA templates 3DOM-PPS-183 (b), 3DOM-PPS-268 (c), 3DOM-PPS-413 (d) and 3DOM-AMPD-444 (e).

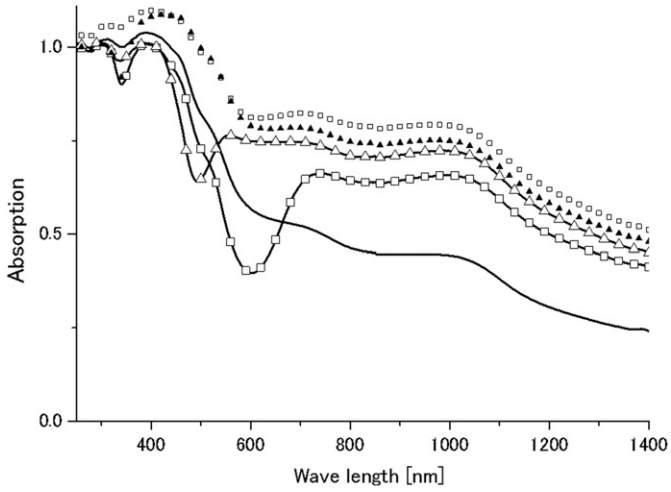

Fig. 6. Reflection spectra of non-porous $LaFeO_3$ prepared without a PMMA template (solid line) and with PMMA templates 3DOM-PPS-183 (open squares), 3DOM-PPS-268 (closed triangles), 3DOM-PPS-413 (solid line with open triangles), and 3DOM-AMPD-444 (solid line with open squares).

oxides. However, observation of photonic stop band of 3DOM mixed metal oxide is a rare example.

3.4. Catalytic activity

Catalytic activity of the 3DOM $LaFeO_3$ for combustion of nanometer size carbon particle was tested using the TG-DTA apparatus, and combustion temperature T_{20} (a temperature where 20 wt% of the carbon was burned) was summarized in Table 1. Nanometer size carbon material is a model of particulate matter exhausted from diesel engines, which cause acute health problems to human beings. $LaFeO_3$ is an active catalyst for the carbon particle combustion [2,5], and we have demonstrated that the introduction of 3DOM structure enhanced the catalytic activity [14]. In the case of 3DOM-PPSs (Entries 1, 2, and 4), catalytic activities are higher than catalytic activity of non-porous $LaFeO_3$, and the catalytic activity is increased by decreasing the PMMA diameter. However, the catalytic activity of 3DOM-AMPDs (Entries 5 and 6) is lower than that of 3DOM-PPSs, and similar to catalytic activity of non-porous $LaFeO_3$. We have found the presence of potassium in 3DOM-PPSs (Entries 1, 2, and 4), which

was included from $K_2S_2O_8$ used as a polymerization initiator. It is known that the presence of potassium increases the catalytic activity [5]. We have prepared non-porous $LaFeO_3$ with potassium (ca. 0.08 wt%) (Table S1), and this non-porous $LaFeO_3$-K showed enhanced catalytic activity similar to the catalytic activities of 3DOM-PPSs (Entry 8). This result indicates that the catalytic activity enhancement is caused by the potassium impurity.

4. Conclusion

Well-ordered 3DOM $LaFeO_3$ materials with pore sizes ranging from 127 to 321 nm were obtained using a colloidal crystal template method in a high pore fraction. Our method uses ethylene glycol–methanol solution of metal nitrates for the metal precursor solution. High porosity and high order of the 3DOM materials, which are attractive features for application as future catalysts, filters, and electrode materials, were confirmed by using SEM, TEM, Hg porosimetry, and photonic stop band properties. Together with our previous papers [16,18], we have demonstrated that our method is a suitable method for preparing 3DOM iron-based oxide including mixed metal oxides.

Acknowledgments

We thank Mr. Kenji Sugawara (High Voltage Electron Microscope Laboratory, Center for Advanced Research of Energy Conversion Materials, Hokkaido University) and Mr. Yoshinobu Nodasaka (Laboratory of Electron Microscopy, Graduate School of Dental Medicine, Hokkaido University) for running TEM measurements. We thank Grants-in-Aid for Scientific Research (Scientific Research "B", No. 18360383) for financial support. We thank Mr. M. Morimoto at Sysmex Corporation (Kobe, Japan) for performing mercury porosimetry.

Appendix A. Supplementary Data

Supplementary data associated with this article can be found in the online version at doi:10.1016/j.jssc.2010.04.012.

References

[1] M.C. Carotta, M.A. Butturi, G. Martinelli, Y. Sadaoka, P. Nunziante, E. Traversa, Sensors Actuators B 44 (1997) 590–594.
[2] D. Fino, N. Russo, G. Saracco, V. Specchia, J. Catal. 217 (2003) 367–375.
[3] R. Spinicci, A. Tofanari, A. Delmastro, D. Mazza, S. Ronchetti, Mater. Chem. Phys. 76 (2002) 20–25.
[4] H. Arai, T. Yamada, K. Eguchi, Y. Seiyama, Appl. Catal. 26 (1986) 265–276.
[5] H. An, C. Kilroy, P.J. McGinn, Catal. Today 98 (2004) 423–429.
[6] X. Qi, J. Zhou, Z. Yue, Z. Gui, L. Li, Ceram. Int. 29 (2003) 347–349.
[7] M. Popa, L.V. Hong, M. Kakihana, Physica B 327 (2003) 233–236.
[8] A.E. Giannakas, A.K. Ladavos, P.J. Pomonis, Appl. Catal. B: Environ. 49 (2004) 147–158.
[9] Y. Sadaoka, H. Aono, E. Traversa, M. Sakamoto, J. Alloys Compd. 278 (1998) 135–141.
[10] E. Traversa, P. Nunziante, M. Sakamoto, Y. Sadaoka, R. Montanari, Mater. Res. Bull. 33 (1998) 673–681.
[11] Assuming that the crystallites are spherical particles, the specific surface area is given by $6000/dA$, where d is density (orthorhombic $LaFeO_3$, 6.64 g cm^{-1}, JCPDS data bank: 37-1493) and A is particle size (nm).
[12] A. Stein, F. Li, N.R. Denny, Chem. Mater. 20 (2008) 649–666.
[13] R.C. Schroden, A. Stein, 3D Ordered Macroporous Material, Wiley-VCH Verlag, Weinheim, Germany, 2004 pp. 465–493.
[14] M. Sadakane, T. Asanuma, J. Kubo, W. Ueda, Chem. Mater. 17 (2005) 3546–3551.
[15] M. Sadakane, C. Takahashi, N. Kato, T. Asamuma, H. Ogihara, W. Ueda, Chem. Lett. 35 (2006) 480–481.
[16] M. Sadakane, C. Takahashi, N. Kato, H. Ogihara, Y. Nodasaka, Y. Doi, Y. Hinatsu, W. Ueda, Bull. Chem. Soc. Jpn. 80 (2007) 677–685.
[17] R.C. Schroden, M. Al-Daous, S. Sokolov, B.J. Melde, J.C. Lytle, A. Stein, M.C. Carbajo, J.T. Fernández, E.E. Rodríguez, J. Mater. Chem. 12 (2002) 3261–3267.
[18] M. Sadakane, T. Horiuchi, N. Kato, C. Takahashi, W. Ueda, Chem. Mater. 19 (2007) 5779–5785.
[19] B.J. Melde, A. Stein, Chem. Mater. 14 (2002) 3326–3331.
[20] W. Dong, H. Bongard, B. Tesche, F. Marlow, Adv. Mater. 14 (2002) 1457–1460.
[21] W. Dong, H. Bongard, F. Marlow, Chem. Mater. 15 (2003) 568–574.
[22] R.C. Schroden, M. Al-Daous, A. Stein, Chem. Mater. 13 (2001) 2945–2950.